



HAL
open science

Spermatozoa methylome and its sensitivity to water temperature in a teleost fish

Aurélien Brionne, Anne-Sophie Goupil, Stéphanie Kica, Jean-Jacques Lareyre, Catherine Labbé, Audrey Laurent

► **To cite this version:**

Aurélien Brionne, Anne-Sophie Goupil, Stéphanie Kica, Jean-Jacques Lareyre, Catherine Labbé, et al.. Spermatozoa methylome and its sensitivity to water temperature in a teleost fish. *Science of the Total Environment*, 2023, 892, pp.164077. 10.1016/j.scitotenv.2023.164077 . hal-04172467

HAL Id: hal-04172467

<https://hal.inrae.fr/hal-04172467v1>

Submitted on 12 Jul 2024

HAL is a multi-disciplinary open access archive for the deposit and dissemination of scientific research documents, whether they are published or not. The documents may come from teaching and research institutions in France or abroad, or from public or private research centers.

L'archive ouverte pluridisciplinaire **HAL**, est destinée au dépôt et à la diffusion de documents scientifiques de niveau recherche, publiés ou non, émanant des établissements d'enseignement et de recherche français ou étrangers, des laboratoires publics ou privés.

1 **SPERMATOZOA METHYLOME AND ITS SENSITIVITY TO WATER TEMPERATURE IN A TELEOST FISH**

2 Aurélien Brionne¹, Anne-Sophie Goupil¹, Stéphanie Kica¹, Jean-Jacques Lareyre¹, Catherine Labbé¹
3 and Audrey Laurent^{1*}

4 ¹INRAE, UR1037 LPGP, Fish Physiology and Genomics, Campus de Beaulieu, F-35000 Rennes, France

5 *corresponding author: audrey.laurent@inrae.fr

6

7 **ABSTRACT**

8 Global climate change and heat waves are sources of stress which fish are facing in the wild as well as
9 in aquaculture context. In coping with important environmental variations, they demonstrate a great
10 plasticity and a tendency for acclimation throughout generations. Here, we question whether fish
11 might be prone to transmit epigenetic alterations through their gametes to their offspring, thus driving
12 rapid environmental adaptation. The question of epigenetic inheritance in fish has become of crucial
13 interest in the recent years, when the mammalian model of methylome erasure in germ cells and
14 embryos was found not to be conserved. In this work, by sequencing spermatozoa after bisulfite
15 conversion, we characterized the methylation landscape of the paternal gamete in rainbow trout (in
16 comparison to muscle) before to demonstrate its sensitivity to a 4°C increased rearing temperature
17 during spermatogenesis. We found that spermatozoa methylome specifically primes housekeeping
18 and developmental genes for activation and might be instrumental to early development. Most of
19 these methylation-free promoters were not affected by temperature, attesting the robustness of the
20 epigenetic programming of early development. However, the increase of temperature triggered the
21 differential methylation of 5,359 regions, among which 560 gene promoters control spermiogenesis
22 and lipid metabolism. We therefore report, for the first time in fish, that sperm epigenetic landscape
23 carries marks of parental thermal living conditions, suggesting that DNA methylation might be a
24 molecular basis of intergenerational inheritance.

25 **KEY WORDS**

26 Spermatozoa, DNA Methylation, Temperature, Inheritance, Fish

27

28 **HIGHLIGHTS**

29 - Rainbow trout sperm methylome is sensitive to temperature

30 - Developmental gene promoters are not affected by a temperature increase

31 - Spermiogenesis and lipid metabolism gene promoters are modulated by a temperature increase

32 - Sperm methylome might be a molecular vector of transgenerational acclimation to environmental
33 change

34

35 **INTRODUCTION**

36 Fish demonstrate a great phenotypic plasticity, which allows them to cope with important
37 environmental variations. At the basis of this plasticity, lies the capacity of the genomes to interact
38 with the environment through epigenetic mechanisms. Epigenetic landscapes indeed regulate cellular
39 transcriptional programs and phenotypes. They rely on DNA methylation and histone post-
40 translational modifications, and are either inherited from a mother cell or modulated upon
41 physiological context.

42 Increasing evidence indicates that epigenetic information, and *a fortiori* its alteration, are
43 transmittable through meiosis and fertilization, from generation to generation. This is particularly
44 suggested by environmental acclimation studies in fish, where offspring performances were shown to
45 be influenced by the life conditions of their genitors. In the tropical reef fish *Acanthochromis*
46 *polyacanthus*, the aerobic scope of individuals raised from hatching to adulthood at higher

47 temperatures (+1.5°C and 3°C) is increased if their parents were also reared at these increased
48 temperatures (Donelson et al., 2012). In the stickleback *Gasterosteus aculeatus*, eggs hatching success
49 and embryo size are influenced by both maternal and paternal exposure to increased temperature
50 (Shama and Wegner, 2014). In the tongue sole *Cynoglossus semilaevis*, thermally-induced sex-reversed
51 pseudo-males have sex-reversed pseudo-male offspring even when these larvae are not exposed to
52 thermal induction (Chen et al., 2014). In the rainbow trout *Oncorhynchus mykiss*, offspring
53 thermotolerance (survival and growth) is improved when genitors also have experienced increased
54 rearing temperature during gametogenesis (Butzge et al., 2021). These data argue in favor of an
55 intergenerational epigenetic inheritance, which suggests that gametes can transmit environmental
56 acclimation clues to the offspring. Very few studies investigated fish gametes epigenetics. So far,
57 Fellous *et al.* reported the differential expression of various epigenetic modifiers in gonads upon
58 increased temperature in stickleback (Fellous et al., 2022), while Gavery *et al.* found in rainbow trout
59 differentially methylated DNA regions in spermatozoa from males of wild versus hatchery origins
60 (Gavery et al., 2018), further indicating that paternal gametes DNA methylome can be modulated by
61 the environment and might be a molecular vector of intergenerational epigenetic inheritance and
62 evolution in fish.

63 Primarily often neglected, the importance sperm DNA methylome for offspring development was
64 recently demonstrated in zebrafish by a series of studies which revealed that, in contrast to
65 mammalian models, embryo DNA methylome is inherited from spermatozoa, maternal DNA
66 methylome being remodeled before zygotic genome activation to match the paternal one (Jiang et al.,
67 2013; Liu et al., 2018; Potok et al., 2013). In addition, zebrafish do not undergo global DNA methylation
68 reprogramming of primordial germ cells, unraveling the persistence of the epigenetic memory
69 throughout generations (Ortega-Recalde et al., 2019). For a better understanding of the molecular
70 basis underlying fish intergenerational inheritance, data reflecting the full diversity of fish species and
71 reproduction modes are missing, and particularly in the omics perspective.

72 Given the potential importance of the paternal methylome in fish and in the context of environmental
73 change, we sought to characterize the rainbow trout (*O. mykiss*) sperm methylome and its sensitivity
74 to a water temperature increase. To this aim, we performed whole genome bisulfite sequencing
75 (WGBS) on sperm DNA of trout reared at 12°C or 16°C during gametogenesis. Our strategy included
76 the sequencing of muscle samples from fish raised at 12°C, which was instrumental to identify
77 spermatozoa-specific DNA methylation profiles. We therefore used these single-base resolution data
78 sets to (i) characterize genome-wide methylation dynamics in representative rainbow trout germline
79 and somatic tissues, (ii) highlight the paternal gamete methylome specificities, (iii) assess its sensitivity
80 to a water temperature increase.

81

82 **RESULTS**

83 **Rainbow trout genome features and WGBS datasets**

84 We briefly summarize here the main features of publicly available rainbow trout genome, which are
85 susceptible to impact DNA methylation. *Oncorhynchus mykiss* genome is made of 2.2 Gb parsed into
86 29 chromosomes with 41,365 and 5,977 coding and non-coding genes, respectively (according to
87 ensembl v105.1 genome annotation of Omyk_1.0 version by Full genebuild). It contains 70,672,452
88 CpGs (70,671,452 nuclear; 1,118 mitochondrial), with a global genome-wide observed over expected
89 (o/e) CpG ratio of 0.8, indicative of a slight CpG erosion during evolution.

90 We performed WGBS of sperm (12 °C and 16°C) and muscle (12°C) DNA samples according to the
91 experimental design presented in **Suppl Fig 1**. WGBS yielded a minimum of 300 million paired-end
92 reads of 150bp per sample (**Tab 1**). In all sample types, the average mapping efficiency of the trimmed
93 reads was of approximately 60%. Our final data set contains 65,125,263 CpGs, representing 92% of the
94 trout genome, 70 to 79 % of them being covered at least 5 x. On average, we obtained a sequencing
95 depth of 10-11 x per strand.

96 We found that almost all methylated cytosines sit in CpG dinucleotides. Indeed, while we measured
97 average methylation of respectively 87.10 and 74.50 % in CpG context in sperm and muscle,
98 respectively, methylated CHG and CHH (H representing A, T or C) were detected at rates lower than
99 1% (**Suppl Tab 1**). For this reason, this study is dedicated to the analysis of CpG methylation only.
100 Finally, we detected very low CpG methylation on mitochondrial DNA, both in muscle and in
101 spermatozoa (**Tab 1**). Our sequencing depth analysis revealed an important mitochondrial DNA over-
102 representation in muscle *versus* sperm (**Tab 1**). This agrees with the expected differences in ratios of
103 nuclear to mitochondrial DNAs between these tissues with abundant mitochondria in muscle while
104 trout spermatozoa possess a unique semicircular mitochondrion.

105 **Supplementary Table 2** recapitulates, for each sample, the number of cytosines in CpG context, being
106 sequenced as methylated in at least one read. When considering the whole data sets, *circa* 93 % of
107 CpGs, in both tissues, showed at least one positive methylation call. Remarkably, these numbers
108 decreased as the coverage threshold applied to the data increased (5 x; 10 x), and they dropped faster
109 in muscle than in spermatozoa. In fact, among the cytosines covered at least 10 times, 67 % of them,
110 on average, were sequenced as methylated in at least one read in muscle, *versus* 85 % in spermatozoa.
111 This very reproducible observation among fish samples reveals a fragment selection bias in the
112 sequencing library preparation process, likely reflecting differences in the chromatin organization
113 between tissues. Non-methylated DNA fragments are more likely to lie in open and accessible
114 chromatin, more prone to be resuspended in solution and to be represented in the sequencing
115 libraries. Both muscle and spermatozoa WGBS libraries show a better representation of non- or poorly-
116 methylated CpGs, but interestingly, this bias is much milder in spermatozoa, reminiscent of a less
117 heterogeneous chromatin conformation in this cell type.

118

119 **Rainbow trout genome is globally methylated both in spermatozoa and muscle**

120 To our knowledge, we present the first comprehensive rainbow trout methylomes of somatic and
121 germline representative cell types. We therefore questioned the general trout DNA methylation
122 pattern in a descriptive analysis of sperm and muscle of fish reared in control condition (**Suppl Fig 1,**
123 **fish 1 to 4**). We first assessed the methylation profile on various genomic features, by calculating the
124 average methylation rates along a reconstituted metagene (**Fig 1A**), around transcription start sites
125 (TSS) and transcription end sites (TES) (**Fig 1B**) of 115,853 annotated Ensembl coding and non-coding
126 transcripts (ensembl v104.1, Omyk_1.0). As already suggested in **Tab 1**, we observed a global DNA
127 hypermethylation of sperm compared to muscle. This result is consistent with the frequently reported
128 high methylation level of spermatozoa in vertebrates (Jiang et al., 2013; Kobayashi et al., 2012; Potok
129 et al., 2013). Nevertheless, both tissues showed a drastic drop of CpG methylation on proximal
130 promoter regions (1kb upstream of TSS) while gene bodies exhibited particularly high methylation
131 rates (**Fig 1 A-B-C**). Repeat elements identified using RepeatMasker (Smit, 2015) were all found to be
132 methylated in both tissues (**Fig 1D**). Transposons, retroposons, LTR, LINEs and SINEs were particularly
133 highly methylated in sperm. Therefore, our analysis of one somatic and one germline tissue showed
134 that, like in most Vertebrates, 5mC in rainbow trout mostly occurs in the CpG dinucleotide context,
135 and shows a global methylation pattern, especially high on gene bodies, and repetitive elements, while
136 gene promoters are more heterogenous and more likely tend to be methylation-free.

137

138 **The signature of sperm methylation profile reflects spermatogenesis and embryonic development**

139 Seeking for spermatozoa methylome specificities we then ran a comparative analysis of sperm and
140 muscle coupled WGBS data (**Suppl Fig 1B, fish 1 to 4**), from fish reared in control condition. A first
141 approach, by principal component analysis (PCA), led us to observe a clear segregation of sperm and
142 muscle samples in spite of a greater dispersion of muscle samples, likely reflecting the greater
143 complexity of this multicellular tissue compared to sperm (**Fig 2A and Suppl Fig 2**).

144 Differentially methylated CpGs (DMCs) between muscle and spermatozoa were identified by DSS
145 (Feng et al., 2014; Wu et al., 2015). We found 36,195,141 DMCs with a threshold adjusted p-value of
146 0.05, meaning that approximately half of the genome is differentially methylated between muscle and
147 spermatozoa. These DMCs are spread over every chromosome (not shown) and across all genomic
148 features (**Fig 2B, C**). As expected, most of DMCs (98 %) are hypermethylated in sperm compared to
149 muscle. Interestingly, while DMCs hypermethylated in spermatozoa are preferentially found in
150 intergenic regions (also representing the largest part of the genome) (**Fig 2B**), the few sperm-specific
151 hypomethylated DMCs, are significantly enriched in gene bodies and promoters. This is indicative of a
152 structural role of sperm DNA hypermethylation on whole genome chromatin. On the contrary, the
153 enrichment, in spermatozoa, of hypomethylated DMCs in genes and gene-proximal sequences
154 suggests that a few promoters specifically escape the global methylation and might be instrumental
155 for the proper execution of spermatogenic transcriptional program. In order to gain insight into this
156 spermatozoon-specific transcriptional regulation, we isolated promoters and compared their
157 methylation levels in both tissues. Promoter methylation status is indeed informative of a
158 transcriptionally repressed or permissive state (however still sensitive to histone post-translational
159 modifications).

160 Common hyper-methylated promoters (53862 transcripts, **Fig 3A**, orange rectangle, **Suppl Tab 3A**)
161 were particularly enriched in GO terms referring to cellular transport, cell adhesion and migration,
162 signaling, response to stimulus, homeostasis, metabolism and terminal differentiation (angiogenesis,
163 pulmonary valve differentiation, melanocyte differentiation).

164 On the other side, 34,925 common hypo-methylated promoters (**Fig 3A**, blue square, **Suppl Tab 3B**)
165 were strongly enriched in GO annotations referring to development (morphogenesis, axis
166 specification, organ development and cell differentiation), germline and housekeeping functions
167 (transcription, translation, metabolism, DNA repair, cell cycle, proliferation, etc). Some signaling,
168 response to stimulus and transport terms also appeared enriched in this category. These data reveal

169 that many genes supporting early development or housekeeping functions are by default in a
170 permissive state for transcription. Even genes which are not necessarily required in the non-
171 proliferative spermatozoa can nevertheless be primed for transcription in order to support embryo
172 development. As an example, TSS region of *pola2*, a gene that encodes a subunit of the DNA
173 polymerase, is equally hypomethylated in both tissues (**Fig 3B**). A vast majority of transcription factors
174 instrumental for development (*otx*, *cbx* or *pax* families) also have constitutively hypo- or low-
175 methylated promoters, even though they are not constitutively expressed. Their expression levels
176 might be regulated by additional post-translational histone modifications as cells differentiate or face
177 particular contexts.

178 Spermatozoa-specific hypo-methylated promoters belonging to 861 transcripts (**Fig 3A**, green shape,
179 **Suppl Tab 3C**) were enriched in spermatozoa specific terms such as meiosis and germline, in addition
180 to development, cellular metabolism and IGF signaling. Some of them are markers of the germline,
181 such as *piwil1* involved in transposable elements silencing during gametogenesis, *dazl* which encodes
182 a master translational regulator during spermatogenesis or the sex determining gene *dmrt1* (**Fig 3B**).
183 Others, such as *spo11* or *mei4* encode specific meiotic recombination factors (**Fig 3B**). We also found
184 the promoters of the pluripotency factors encoding *klf4* (**Fig 3B**) and *esrrb* to be specifically
185 hypomethylated. Noticeably, a subset of developmental factors escapes constitutive hypomethylation
186 and is specifically reprogrammed to be hypomethylated in the spermatozoa. This is the case of the
187 entire *hox* clusters (**Fig 3B**), in which remarkably, altogether promoters: gene bodies and intergenic
188 regions, spanning hundreds of kilobases are fully demethylated. The conserved *mir10b*, lying in the
189 vicinity of *hox4* paralogs and co-expressed during development is therefore hypo-methylated as well.
190 Interestingly *meis1a* (**Fig 3B**) or *meis3*, which are *hox* cofactors involved in axis patterning and organ
191 morphogenesis, are also specifically hypomethylated in the spermatozoa. This set of spermatozoa-
192 specific genes is then silenced by methylation in the adult differentiated muscle, meaning that they
193 might be sensitive to a dynamic regulation by promoter methylation.

194 Finally, 632 muscle-specific hypo-methylated promoters (**Fig 3A**, red shape, **Suppl Tab 3D**) were
195 enriched in terms referring to terminal differentiation, muscle and vasculature function, cellular
196 metabolism, response to stimulus and immune response. These dynamic promoters have undergone
197 a demethylation during differentiation and are likely to be controlling muscle function. They mainly
198 regulate terminal differentiation genes, such as *plecb* encoding a skeletal muscle plectin or signaling
199 molecules such as *rarg* encoding a retinoic acid receptor (**Fig 3B**).

200 Altogether this work strongly supports the idea that sperm methylome is carrying an epigenetic
201 program, which might be instrumental for both spermatogenesis and proper embryo development.

202

203 **Increasing rearing temperature alters sperm methylome**

204 Given the importance of the paternal methylome in fish, we sought to question its robustness or
205 sensitivity to environmental conditions. We chose to evaluate the potential impact of an increased
206 rearing water temperature during gametogenesis on rainbow trout spermatozoa methylome. To this
207 aim, we analyzed by WGBS the sperm of 6 fish bred at 16°C from May to November versus 6 control
208 fish kept at 12°C (**Tab 1**, **Suppl Fig 1B**). Global average methylation rates were similar in both conditions
209 (**Suppl Tab 1**) and the PCA analysis did not show any strong segregation between 12°C and 16°C
210 spermatozoa samples (**Fig 4A and Suppl Fig 2**). Nevertheless, we identified 112,386 DMCs with a
211 threshold adjusted p-value of 0.05 (**Fig 4B**). Nearly 50% of DMCs were hypomethylated (55,738) and
212 50% hypermethylated (56,648) at 16°C compared to 12°C. Interestingly, we found that 92% of these
213 DMCs fall into differentially methylated regions (DMRs). This result indicates that an increase of rearing
214 water temperature during gametogenesis alters spermatozoa methylome in a non-sporadic and non-
215 random way. The affected cytosines instead concentrate into 5,359 DMRs of 400 bp median length
216 resulting from a coordinated response to temperature increase. Ten % of these DMRs affect
217 promoters, later on designed as prom-DMRs. Noteworthy, very few of these differentially methylated
218 promoters had been previously identified as tissue specific, i.e. hypomethylated exclusively in either

219 spermatozoa or muscle (11 and 7, respectively) (**Fig 5A**). On the contrary, they mostly fall in the
220 common hypo-, common hyper- or common moderately-methylated promoter categories, already
221 indicating that developmental genes epigenetically reprogrammed in the spermatozoa were mostly
222 unaffected.

223 In order to thoroughly study the biological functions of the differentially methylated promoters (prom-
224 DMRs), we carried out both (i) a non-biased search for GO terms enrichment, (ii) a manual examination
225 and annotation of the TOP 200 differentially methylated ones. Both approaches were mainly based on
226 gene orthologies and mammalian literature. Examples of hypo- and hyper-methylated gene promoters
227 and enriched GO categories are indicated in **Fig 5A**, **Suppl Tab 4 A-B** and **Suppl Tab 5**. Interestingly, the
228 manual annotation analysis largely confirmed the GO term enrichment test and indicated that the
229 prom-DMRs impacted spermiogenesis and lipid metabolism genes, leaving most developmental genes
230 unaffected.

231

232 *Intracellular vesicle trafficking*

233 We found prom-DMRs annotations covering virtually the whole spectrum of the molecular
234 components regulating vesicular trafficking and/or autophagy: from plasma and organelle membrane
235 regulation to motor proteins and signaling (**Fig 5A**, **Suppl Tab 5**). We found DMRs in the promoters of
236 *asah2* (N-AcylSphingosine AmidoHydrolase) (**Fig 5B**), *ppm1la* and *cert1* (ceramide transporters), *sphk1*
237 (sphingosine kinase) and *mdga1* (MAM Domain containing Glycosylphosphatidylinositol Anchor),
238 which regulate membrane ceramid and sphingolipid metabolism, therefore affecting membrane
239 properties, lipid rafts, protein sorting, signaling, plasma membrane curvature and endocytosis
240 initiation (Pepperl et al., 2013; Tani et al., 2007; Young and Wang, 2018). The promoter of the
241 membrane receptor *s1pr3* (protein-G-coupled receptor of Phospho-Sphingosine) is differentially
242 methylated as well as the promoters of *vldlr* and *mesd* (very low density lipoprotein receptor and
243 chaperone for low density lipoprotein receptors (LRP), respectively), likely affecting endocytosis

244 initiation. We found several promoters of signaling molecules regulating vesicular traffic such as *grb2b*,
245 *praf2* and *sh3gl1b* (adaptors), *rab1b* and *rnd2* (small GTPases), *dennd5a*, *rgl2*, *arhgef18a*, *quo*, *fgd4b*
246 and *trappc13* (GEF, guanine nucleotide exchange factors for small GTPases), and *git2a*, *tbc1d2* and
247 *rgs3b* (GAP, GTPases activating proteins). DMRs also affected promoters of vesicular traffic effectors
248 such as the motor myosin *myo5b* (**Fig 5B**), the actin interacting WASP family member *wasf3a* and the
249 kinesin *kif26ba*. Finally, we found prom-DMRs potentially affecting the regulation of membrane fusion,
250 such as the promoters of *nsfl1c* (*p47* ortholog) and *nsfb* (*nsf* ortholog) (**Fig 5B**) encoding representative
251 actors of the two major membrane fusion pathways (NSF and VCP/p47 pathways) (Brunger and
252 DeLaBarre, 2003), the promoter of *rnf126* (E3 ubiquitin ligase, which is essential for proteasomal
253 degradation in the VCP/p47 pathway) (**Fig 5B**), or the promoter of *myofl* involved in membrane fusion
254 and repair. Markers of various types of intracellular vesicles were found differentially methylated,
255 such as *ap5b1* and *ap5s1*, encoding two subunits of the late endosome AP-5 adaptor complex,
256 *trappc13* encoding a component of the trafficking particle protein complex and *vmp1* (vacuole
257 membrane protein), both involved in secretion and autophagy, therefore suggesting that several
258 pathways orchestrating cellular trafficking might be elicited in response to increased rearing
259 temperature. Therefore, sperm cells exposed to increased temperature exhibit a differential
260 methylation at numerous promoters regulating vesicular trafficking potentially involving protein
261 folding and degradation, cell signaling, autophagy or apoptosis.

262

263 *Cytoskeleton remodeling*

264 We found abundant prom-DMRs indicative of a reorganization of the cytoskeleton, mostly affecting
265 actin network, cell-cell and cell-extra cellular matrix (ECM) adhesion (**Fig 5A, Suppl Tab 5**). As such, we
266 found promoters of genes controlling actin dynamics: *flna* (filamin a) (**Fig 5B**), *tmod1* (tropomodulin)
267 (**Fig 5B**), *add2* (adducin), *coro1b* (coronin) and *prkd4* (kinase) (**Fig 5B**), are all reported to interact with
268 actin network and/or control its assembly, filament elongation or depolymerization. In addition,

269 *sema4gb*, encoding a semaphorin was found among the prom-DMRs (**Fig 5B**). Semaphorins regulate
270 intra-cellular actin filaments and microtubule network interactions with the ECM. Interestingly, in the
271 same pathway, the promoters of the semaphorin receptors *plkdc2* (plexin) and *nrp1a* (neurpilin) and
272 its co-factor *rftn2* (raftlin) were also differentially methylated. Other promoters of genes encoding
273 components of cellular junctions or cell-ECM adhesion complexes were found among DMRs, such as
274 the protocadherins *pcdh1g32* and *pcdhb*, and the cadherin interacting angiomin-like *amotl2a*
275 (adherens junctions), *nectin1a* (adherens junctions), the claudin encoding *clnd* and *clnd23a* (tight
276 junctions). Finally, other prom-DMRs were reported in the literature to be regulators of cell-cell and
277 cell-ECM adhesion, such as *susd2*, *mpp3b*, *sh3bgrl*, *tbc1d2*, *mdga2a*, *cadm1b* and *rxylt1*. These results
278 highlight a high occurrence of genes related to actin cytoskeleton remodeling, cell-cell and cell-ECM
279 adhesion, among promoters affected by an increased temperature in spermatozoa. This suggests a
280 potential response of differentiating germ cells at the level of both intra- and inter-cellular processes.

281 Therefore, numerous prom-DMRs annotations converge toward a functional adaptation of germ cells
282 to a temperature stress with a coordinated cytoskeletal reorganization supporting an important
283 modulation of intracellular vesicular trafficking and autophagy. This could be interpreted as a
284 conserved and generic cytoprotective response to heat stress. Similar results were indeed reported by
285 Madeira *et al.* who observed that larvae of sea bream *Sparus aurata* modulate, at the protein level,
286 the intracellular transport, protein folding and degradation and the cytoskeleton dynamics pathways
287 in response to temperature stress (Madeira *et al.*, 2016). Indications of cytoskeleton remodeling in
288 adaptation to increased temperature were also observed in a blue mussel gills (Fields *et al.*, 2012) or
289 in the myofibril tissue of the crab *P. cinctipes* (Garland *et al.*, 2015). During their progression, male
290 germ cells in rainbow trout thus modulate promoters classically involved in somatic heat stress
291 adaptation and keep traces of these alterations in the terminally differentiated spermatozoa.

292

293 *Spermiogenesis*

294 Beyond the activation of possibly pan cell type adaptive mechanisms to increased rearing temperature,
295 the cellular trafficking and cytoskeleton actors differentially methylated in our study interestingly
296 pinpoint one major function precluding the spermatozoon stage: spermiogenesis. In the testis,
297 differentiating sperm cells undergo drastic cell shape and cell-cell adhesion remodeling. These
298 processes result from a tight control of the cytoskeleton dynamics and a recycling of intercellular
299 junctions and ECM-interacting receptors at the plasma membrane, processes which are in turn
300 dependent on endocytosis, vesicle trafficking, autophagy and protein recycling. Indeed, proper Golgi
301 orientation, cytoskeleton, membrane fusion and vesicular trafficking are essential for the formation of
302 the acrosome. Rainbow trout spermatozoa possess a transitory pseudo-acrosomal vesicle which is
303 visible at the round spermatid stage and only leaves a cytoskeletal scar at later stages, reminiscent of
304 mammalian acroplaxome (Billard, 1983). Endocytosis and vesicle trafficking are also crucial to the
305 intraflagellar vesicle transport of molecules allowing the growth of the flagellum, and later on, for the
306 elimination of the cytoplasm in late spermiogenesis and the individualization of sperm cells from the
307 syncytium for spermiation. These spermiogenetic processes might recruit and coordinate common
308 actors of vesicular trafficking expressed during spermiogenesis. It is therefore tempting to speculate
309 that several gene promoters instrumental for spermiogenesis have been targeted by differential
310 methylation. Interestingly, we found *tmf1* in the list of differentially methylated promoters (**Fig 5B**). Its
311 mouse ortholog TMF/ARA160 encodes a protein associated to Golgi, emerging vesicles and
312 microtubule network, which KO in male germ cells induces Golgi misorientation, lack of homing of pro-
313 acrosomal vesicles, agenesis of the acrosome, inefficient cytoplasm removal and misshapen sperm
314 head (Elkis et al., 2015; Lerer-Goldshtein et al., 2010). Myosin VI and Myosin Va, orthologs of *myo5b*,
315 which we found differentially methylated in our data set, are essential for acrosome formation in the
316 mouse and in the Chinese mitten crab (*E. sinensis*), respectively (Sun et al., 2010; Zakrzewski et al.,
317 2020). The small GTPase *rnd2* mentioned earlier (“intracellular vesicle trafficking section”) was
318 detected in Golgi and pro-acrosomal vesicles of rat spermatids (Naud et al., 2003).

319 In addition, several promoters of genes specifically implicated in other aspects spermatogenesis were
320 found differentially methylated. As such, *rad51ap1* (**Fig 5B**), *rec8b* and *rmi2* (**Fig 5B**) encode essential
321 actors of the meiotic homologous recombination (Bommi et al., 2019; Dray et al., 2011; Pires et al.,
322 2017; Velkova et al., 2021), *aurka* encodes the aurora A kinase, involved in centrosome maturation
323 and spindle formation during mitosis and also found to be essential for meiosis and spermiogenesis in
324 mice (Lester et al., 2021), and *mief* (**Fig 5B**) encodes in human a mitochondrial fusion factor (Zhao et
325 al., 2011), reminiscent of the mitochondrial remodeling to which rainbow trout spermatozoa are
326 subjected during their differentiation. Interestingly, while autophagy is involved in spermiogenesis,
327 and in particular in acrosome formation in mice (Wang et al., 2014), its increase in the human
328 pathological model of cryptorchidism is associated to an impairment of spermatozoa maturation
329 (Yefimova et al., 2019). Remarkably, in spite of the wide variation in spermatozoa morphologies and
330 action modes among animals, cytoskeleton remodeling, vesicle trafficking and autophagy seem to be
331 part of common pathways regulating normal, adaptive or pathological male germ cell maturation
332 (White-Cooper and Bausek, 2010). Prom-DMRs which we detected in our experimental contrast are
333 enriched in these GO categories. Altogether, these results argue in favor of an altered regulation of
334 the late spermatogenic program (meiotic and post-meiotic) upon increased temperature. This could
335 suggest that regions of the genome which were active during the exposure of the fish to the
336 temperature stress (orchestrating late spermatogenesis) were more particularly prone to undergo a
337 modulation of their methylation level.

338

339 *Lipid metabolism*

340 Interestingly, a third category of abundant prom-DMR annotations relates to the regulation of lipid
341 metabolism (**Fig 5A, Suppl Tab 5**). We found several promoters of lipid catabolism genes such as *asah2*
342 (ceramidase), *daglb* (lipase) or *abcd3a* (encoding a transporter involved in peroxisomal transport or
343 catabolism of very long chain fatty acids). The regulation of long chain fatty acid metabolism was more

344 specifically affected with the differential promoter methylation of *cox-1* (cyclooxygenase involved in
345 arachidonic acid conversion) (**Fig 5B**), *ptges* (terminal enzyme of the cox-2-mediated prostaglandin E2
346 biosynthesis from arachidonic acid), *gstp1* (glutathione S-transferase), *gpx1* (glutathione peroxidase)
347 and *elovl7b* (fatty acid elongase) (**Fig 5B**). In addition, the promoter of *gps2* (**Fig 5B**), which encodes a
348 PPAR γ transcriptional co-activator, was found differentially methylated. Fatty acid composition in
349 testis was shown to be of particular relevance for sperm maturation and function in human (Collodel
350 et al., 2020), in ruminant (Van Tran et al., 2017), or rooster (Teymouri Zadeh et al., 2020). PPAR γ ,
351 known to be master regulator of adipocyte differentiation and lipid metabolism, was also shown to
352 control fatty acid metabolism in human and therefore suspected to be instrumental for proper sperm
353 formation (Olia Bagheri et al., 2021). Finally, the promoter of *hnf4a*, which controls fatty acid oxidation
354 and metabolism in hepatocytes, was overlapping with a DMR in our analysis (**Fig 5B**). The appearance
355 of fatty acid metabolism as a potentially altered pathway, controlled by PPAR γ and/or Hnf4a, could be
356 interpreted as a metabolic adaptation of poikilotherm fish to temperature. The activity of several
357 desaturases, elongases and fatty acid composition where indeed shown to be sensitive to temperature
358 in fish and rainbow trout in particular (Tocher et al., 2004). It is remarkable however to find its scar in
359 the methylation profile of spermatozoa.

360

361 **CONCLUSION**

362 In the present study, we aimed at characterizing the rainbow trout sperm methylome (using muscle as
363 a somatic reference tissue) and its sensitivity to a rearing temperature increase of 4°C during
364 spermatogenesis. Single-base resolution methylomes revealed that an important pool of gene
365 promoters is methylation-free in spermatozoa, and therefore in a permissive state for transcription,
366 although sperm DNA is tightly packed and transcriptionally silent. Sperm cells thus carry an epigenetic
367 code seemingly resulting from history and preparing their future role. Remarkably, sperm methylation-
368 free promoters control housekeeping, early development and germline functions.

369 We found that an increased rearing temperature during spermatogenesis significantly impacted sperm
370 methylome. Interestingly, DMRs affected promoters controlling spermiogenesis and lipid metabolism
371 genes, leaving most developmental genes unaffected. This organized response to heat stress suggests
372 a coordination by a signaling pathway. Our data highlighted PPAR γ and Hnf4 pathways. Alternatively,
373 some genomic regions might be more prone to undergo methylome alterations because of a pre-
374 established sensitivity, laying in the fact that they are active during spermiogenesis, which is both a
375 period of deep chromatin remodeling and the time of experimental stress exposure. In an attempt to
376 identify a potential driver of the differential methylation we observed, we looked for enriched
377 transcription factor binding sites (TFBS) in our DMR using MEME suite. Interestingly, the most
378 significantly enriched TFBS was the one of PRDM9 (**Suppl Fig 3**), which binds to recombination hotspots
379 during meiosis. This opens the seducing possibility that meiotic recombination sites are at particular
380 risk of epigenetic reprogramming upon environmental stress. Taken together, for the first time in
381 rainbow trout, our results demonstrate that the methylation status of sperm-specific gene promoters
382 controlling housekeeping and developmental function is very robust in the context of a 4°C
383 temperature increase during spermatogenesis. Remarkably however, we found that the sperm
384 methylome is altered and carry the traces of the life history of the individuals. We found epigenetic
385 alterations of spermiogenesis and lipid metabolism controlling genes, which will be transmitted to the
386 next generation. Future investigation should answer whether this altered sperm epigenome could be
387 a molecular basis of acclimation to a heat stress for next generations and whether it could impact
388 positively or negatively offspring performances under various conditions.

389

390

391

392

393 MATERIAL AND METHODS

394 Ethics statements

395 The experiment was conducted following the Guidelines of the National Legislation on Animal Care of
396 the French Ministry of Research (Decree No 2013–118, February 2013) and in accordance with EU legal
397 frameworks related to the protection of animals used for scientific purposes (i.e., Directive
398 2010/63/EU). The scientists in charge of the experiments received training and personal authorization.
399 The experiment was conducted at the INRAE Physiology and Genomic Laboratory (LPGP) experimental
400 facilities (permit number C35-238-6, Rennes, France), and approved by the ethics committee for the
401 animal experimentation of Rennes under the authorization number T-2019-05-AL.

402

403 Fish rearing and sampling

404 *Oncorhynchus mykiss* rainbow trouts, from a winter spawning strain (December 15 – January 15), were
405 reared in our experimental farm (river water, in which temperatures are near 7.5°C in winter and can
406 reach 20°C in summer). Two groups of 20 males were transferred to our indoor fish facility in April
407 (April 4th 2019) of their second year, when they reached 15 months of age. They were kept in a recycling
408 system, under artificial spring/summer/autumn photoperiod, and at the temperatures of 12°C and
409 16°C (after 2 weeks acclimation and gradual temperature increase, from April 18th 2019 till sample
410 collection). Regarding the reproductive cycle, this period of experimental exposure corresponds to the
411 post-meiotic phase. For each experimental group, fish were split into two water tanks (10 fish per
412 tank). The growth of the fish in both groups was recorded and their commercial diet rations were
413 adapted so that both groups follow similar growth curves (Supplementary Figure 4). Fish were checked
414 every two weeks for milt production, at the occasion of the measure of their individual weight. Sperms
415 were harvested by stripping (first spermiation) and muscle samples were taken after euthanasia
416 (tricaine 200 mg/mL).

417 **Whole genome bisulfite sequencing**

418 We analyzed by WGBS and compared (i) the sperm of 4 fish bred at 12°C *versus* the muscle of the same
419 4 fish (reared in control condition), and (ii) the sperm of 6 fish bred at 16 °C from mid-April to November
420 *versus* 6 control fish kept at 12°C (**Tab 1, Suppl Fig 1B**). Genomic DNA was prepared after an overnight
421 lysis in TNES/Urea buffer (10 mM Tris, 0.125 M NaCl, 10 mM EDTA, 17 mM SDS, 4M urea, pH 8)
422 complemented with 80ug/mL proteinase K at 42°C. After phenol-chloroform extraction, the samples
423 were treated with RNase A (4mg/mL) and gDNAs were precipitated by the addition of isopropanol and
424 sodium acetate. Whole genome bisulfite sequencing libraries were prepared (according to Accel-NGS
425 Methyl-Seq DNA library Kit for Illumina protocol, Swift Biosciences) and sequenced in 150 bp paired-
426 end reads by Novogene company.

427

428 **Bio-informatic analysis**

429 WGBS yielded a minimum of 300 million paired-end 150 bp reads per sample (Tab 1). Quality and
430 adapter trimming of the reads was carried out using Trim Galore (with an additional 10 bp clipping for
431 read2 5'-end and read1 3'-end) (Krueger and Galore, n.d.). After trimming, only uniquely mapped reads
432 on the *O. mykiss* genome or its *in silico* bisulfite converted version were kept for further analysis (using
433 Bismark bio-informatic software and Omyk_1.0 genome version, (Krueger and Andrews, 2011)).
434 BigWig files were obtained with bedGraphToBigWig (Kent et al., 2010) and methylation values were
435 visualized with Integrative Genome Viewer (Robinson et al., 2011). These steps were included in a
436 workflow which agrees to FAIR principles and is accessible online
437 (<https://forgemia.inra.fr/lpgp/methylome>). The methylome (v1.0) workflow was built in Nexflow dsl2
438 language using a singularity container and optimized in terms of computing resources (cpu, memory)
439 for its use on an informatic farm with a slurm scheduler.

440 Differentially methylated cytosines (DMCs) were identified by the R package DSS (Feng et al., 2014;
441 Wu et al., 2015), using the optional methylation level smoothing on 500 bp and a Benjamini-Hochberg
442 adjusted p-value threshold of 0.05. Differentially methylated regions (DMRs) were defined using DSS
443 package with seed regions containing at least 5 CpGs and expansion window criterias agreeing with a
444 minimum of 75 % of DMCs (with raw pval < 0.01).

445 CpGs were annotated with GenomeFeatures (Brionne, n.d.), RepeatMasker (Smit, 2015) and ensembl
446 v105.1 annotation. Biological interpretations were carried out using ViSEAGO R package (Brionne et
447 al., 2019) and the Gene Ontology (GO) public database. Associated gene terms were implemented
448 from the extended Ensembl Compara custom annotation based on the release 103. Enrichment tests
449 were performed using exact Fisher's test. Enriched GO terms (p-val < 0.01) were grouped into
450 functional clusters by Wang's semantic similarity respecting GO graph topology and Ward's criterion.

451

452 **AVAILABILITY OF DATA**

453 The data that support the findings are already deposited and will be available on the ENA archive
454 (<https://www.ebi.ac.uk/ena/browser/home>) under the accession number (PRJEB56697) and following
455 an embargo from the date of publication. They can be transferred to the reviewers upon editor
456 request.

457

458 **ACKNOWLEDGEMENTS**

459 The study was funded by the department of animal physiology (PHASE) of INRAE (ACI 2019). We thank
460 Julien Bobe for its contribution to the experimental design and his comments on the manuscript. We
461 thank the staff of our experimental farm (PEIMA, INRAE) and fish facility (ISC LPGP) and particularly
462 Cécile Duret for dedicated handling of our experimental fish.

463

464 **AUTHORS CONTRIBUTIONS STATEMENT**

465 AL designed the project and experiments, supervised the study and wrote the manuscript. CL and JLL
466 contributed to the design of the project. ASG, SK and CL performed the wet lab work. AB performed
467 the bio-informatic analysis. All the authors read and approved the manuscript.

468

469 **REFERENCES**

- 470 Billard, R., 1983. Spermiogenesis in the rainbow trout (*Salmo gairdneri*). An ultrastructural study. *Cell*
471 *Tissue Res.* 233, 265–284. <https://doi.org/10.1007/BF00238295>
- 472 Bommi, J.R., Rao, H.B.D.P., Challa, K., Higashide, M., Shinmyozu, K., Nakayama, J.-I., Shinohara, M.,
473 Shinohara, A., 2019. Meiosis-specific cohesin component, Rec8, promotes the localization of
474 Mps3 SUN domain protein on the nuclear envelope. *Genes Cells Devoted Mol. Cell. Mech.*
475 24, 94–106. <https://doi.org/10.1111/gtc.12653>
- 476 Brionne, A., n.d. GenomeFeatures: A convenient tool for multiple genomic features annotations.
- 477 Brionne, A., Juanchich, A., Hennequet-Antier, C., 2019. ViSEAGO: a Bioconductor package for
478 clustering biological functions using Gene Ontology and semantic similarity. *BioData Min* 12,
479 16.
- 480 Brunger, A.T., DeLaBarre, B., 2003. NSF and p97/VCP: similar at first, different at last. *FEBS Lett.* 555,
481 126–133. [https://doi.org/10.1016/s0014-5793\(03\)01107-4](https://doi.org/10.1016/s0014-5793(03)01107-4)
- 482 Butzge, A.J., Yoshinaga, T.T., Acosta, O.D.M., Fernandino, J.I., Sanches, E.A., Tabata, Y.A., de Oliveira,
483 C., Takahashi, N.S., Hattori, R.S., 2021. Early warming stress on rainbow trout juveniles
484 impairs male reproduction but contrastingly elicits intergenerational thermotolerance. *Sci.*
485 *Rep.* 11, 17053. <https://doi.org/10.1038/s41598-021-96514-1>
- 486 Chen, S., Zhang, G., Shao, C., Huang, Q., Liu, G., Zhang, P., Song, W., An, N., Chalopin, D., Volff, J.-N.,
487 Hong, Y., Li, Q., Sha, Z., Zhou, H., Xie, M., Yu, Q., Liu, Y., Xiang, H., Wang, N., Wu, K., Yang, C.,
488 Zhou, Q., Liao, X., Yang, L., Hu, Q., Zhang, Jilin, Meng, L., Jin, L., Tian, Y., Lian, J., Yang, J., Miao,
489 G., Liu, S., Liang, Z., Yan, F., Li, Y., Sun, B., Zhang, H., Zhang, Jing, Zhu, Y., Du, M., Zhao, Y.,
490 Schartl, M., Tang, Q., Wang, J., 2014. Whole-genome sequence of a flatfish provides insights
491 into ZW sex chromosome evolution and adaptation to a benthic lifestyle. *Nat. Genet.* 46,
492 253–260. <https://doi.org/10.1038/ng.2890>
- 493 Collodel, G., Castellini, C., Lee, J.C.-Y., Signorini, C., 2020. Relevance of Fatty Acids to Sperm
494 Maturation and Quality. *Oxid. Med. Cell. Longev.* 2020, 7038124.
495 <https://doi.org/10.1155/2020/7038124>
- 496 Donelson, J.M., Munday, P.L., McCormick, M.I., Pitcher, C.R., 2012. Rapid transgenerational
497 acclimation of a tropical reef fish to climate change. *Nat. Clim. Change* 2, 30–32.
498 <https://doi.org/10.1038/nclimate1323>
- 499 Dray, E., Dunlop, M.H., Kauppi, L., San Filippo, J., Wiese, C., Tsai, M.-S., Begovic, S., Schild, D., Jasin,
500 M., Keeney, S., Sung, P., 2011. Molecular basis for enhancement of the meiotic DMC1
501 recombinase by RAD51 associated protein 1 (RAD51AP1). *Proc. Natl. Acad. Sci. U. S. A.* 108,
502 3560–3565. <https://doi.org/10.1073/pnas.1016454108>

503 Elkis, Y., Bel, S., Rahimi, R., Lerer-Goldstein, T., Levin-Zaidman, S., Babushkin, T., Shpungin, S., Nir, U.,
504 2015. TMF/ARA160 Governs the Dynamic Spatial Orientation of the Golgi Apparatus during
505 Sperm Development. *PloS One* 10, e0145277. <https://doi.org/10.1371/journal.pone.0145277>
506 Fellous, A., Wegner, K.M., John, U., Mark, F.C., Shama, L.N.S., 2022. Windows of opportunity: Ocean
507 warming shapes temperature-sensitive epigenetic reprogramming and gene expression
508 across gametogenesis and embryogenesis in marine stickleback. *Glob. Change Biol.* 28, 54–
509 71. <https://doi.org/10.1111/gcb.15942>
510 Feng, H., Conneely, K.N., Wu, H., 2014. A Bayesian hierarchical model to detect differentially
511 methylated loci from single nucleotide resolution sequencing data. *Nucleic Acids Res* 42, e69.
512 Fields, P.A., Zuzow, M.J., Tomanek, L., 2012. Proteomic responses of blue mussel (*Mytilus*) congeners
513 to temperature acclimation. *J. Exp. Biol.* 215, 1106–1116.
514 <https://doi.org/10.1242/jeb.062273>
515 Garland, M.A., Stillman, J.H., Tomanek, L., 2015. The proteomic response of cheliped myofibril tissue
516 in the eurythermal porcelain crab *Petrolisthes cinctipes* to heat shock following acclimation
517 to daily temperature fluctuations. *J. Exp. Biol.* 218, 388–403.
518 <https://doi.org/10.1242/jeb.112250>
519 Gavery, M.R., Nichols, K.M., Goetz, G.W., Middleton, M.A., Swanson, P., 2018. Characterization of
520 Genetic and Epigenetic Variation in Sperm and Red Blood Cells from Adult Hatchery and
521 Natural-Origin Steelhead, *Oncorhynchus mykiss*. *G3 Bethesda Md* 8, 3723–3736.
522 <https://doi.org/10.1534/g3.118.200458>
523 Jiang, L., Zhang, Jing, Wang, J.-J., Wang, L., Zhang, L., Li, G., Yang, X., Ma, X., Sun, X., Cai, J., Zhang,
524 Jun, Huang, X., Yu, M., Wang, X., Liu, F., Wu, C.-I., He, C., Zhang, B., Ci, W., Liu, J., 2013.
525 Sperm, but not oocyte, DNA methylome is inherited by zebrafish early embryos. *Cell* 153,
526 773–784. <https://doi.org/10.1016/j.cell.2013.04.041>
527 Kent, W.J., Zweig, A.S., Barber, G., Hinrichs, A.S., Karolchik, D., 2010. BigWig and BigBed: enabling
528 browsing of large distributed datasets. *Bioinformatics* 26, 2204–2207.
529 Kobayashi, H., Sakurai, T., Imai, M., Takahashi, N., Fukuda, A., Yayoi, O., Sato, S., Nakabayashi, K.,
530 Hata, K., Sotomaru, Y., Suzuki, Y., Kono, T., 2012. Contribution of intragenic DNA methylation
531 in mouse gametic DNA methylomes to establish oocyte-specific heritable marks. *PLoS Genet.*
532 8, e1002440. <https://doi.org/10.1371/journal.pgen.1002440>
533 Krueger, F., Andrews, S.R., 2011. Bismark: a flexible aligner and methylation caller for Bisulfite-Seq
534 applications. *Bioinforma. Oxf. Engl.* 27, 1571–1572.
535 <https://doi.org/10.1093/bioinformatics/btr167>
536 Krueger, F., Galore, T., n.d. A wrapper tool around Cutadapt and FastQC to consistently apply quality
537 and adapter trimming to FastQ files.
538 Lerer-Goldshtein, T., Bel, S., Shpungin, S., Pery, E., Motro, B., Goldstein, R.S., Bar-Sheshet, S.I.,
539 Breitbart, H., Nir, U., 2010. TMF/ARA160: A key regulator of sperm development. *Dev. Biol.*
540 348, 12–21. <https://doi.org/10.1016/j.ydbio.2010.07.033>
541 Lester, W.C., Johnson, T., Hale, B., Serra, N., Elgart, B., Wang, R., Geyer, C.B., Sperry, A.O., 2021.
542 Aurora A Kinase (AURKA) is required for male germline maintenance and regulates sperm
543 motility in the mouse. *Biol. Reprod.* 105, 1603–1616. <https://doi.org/10.1093/biolre/ibab168>
544 Liu, G., Wang, W., Hu, S., Wang, X., Zhang, Y., 2018. Inherited DNA methylation primes the
545 establishment of accessible chromatin during genome activation. *Genome Res.* 28, 998–
546 1007. <https://doi.org/10.1101/gr.228833.117>
547 Madeira, D., Araújo, J.E., Vitorino, R., Capelo, J.L., Vinagre, C., Diniz, M.S., 2016. Ocean warming alters
548 cellular metabolism and induces mortality in fish early life stages: A proteomic approach.
549 *Environ. Res.* 148, 164–176. <https://doi.org/10.1016/j.envres.2016.03.030>
550 Naud, N., Touré, A., Liu, J., Pineau, C., Morin, L., Dorseuil, O., Escalier, D., Chardin, P., Gacon, G., 2003.
551 Rho family GTPase Rnd2 interacts and co-localizes with MgcRacGAP in male germ cells.
552 *Biochem. J.* 372, 105–112. <https://doi.org/10.1042/BJ20021652>
553 Olia Bagheri, F., Alizadeh, A., Sadighi Gilani, M.A., Shahhoseini, M., 2021. Role of peroxisome
554 proliferator-activated receptor gamma (PPAR γ) in the regulation of fatty acid metabolism

555 related gene expressions in testis of men with impaired spermatogenesis. *Reprod. Biol.* 21,
556 100543. <https://doi.org/10.1016/j.repbio.2021.100543>

557 Ortega-Recalde, O., Day, R.C., Gemmell, N.J., Hore, T.A., 2019. Zebrafish preserve global germline
558 DNA methylation while sex-linked rDNA is amplified and demethylated during feminisation.
559 *Nat. Commun.* 10, 3053. <https://doi.org/10.1038/s41467-019-10894-7>

560 Pepperl, J., Reim, G., Lüthi, U., Kaech, A., Hausmann, G., Basler, K., 2013. Sphingolipid depletion
561 impairs endocytic traffic and inhibits Wingless signaling. *Mech. Dev.* 130, 493–505.
562 <https://doi.org/10.1016/j.mod.2013.04.001>

563 Pires, E., Sung, P., Wiese, C., 2017. Role of RAD51AP1 in homologous recombination DNA repair and
564 carcinogenesis. *DNA Repair* 59, 76–81. <https://doi.org/10.1016/j.dnarep.2017.09.008>

565 Potok, M.E., Nix, D.A., Parnell, T.J., Cairns, B.R., 2013. Reprogramming the maternal zebrafish
566 genome after fertilization to match the paternal methylation pattern. *Cell* 153, 759–772.
567 <https://doi.org/10.1016/j.cell.2013.04.030>

568 Robinson, J.T., Thorvaldsdóttir, H., Winckler, W., Guttman, M., Lander, E.S., Getz, G., Mesirov, J.P.,
569 2011. Integrative genomics viewer. *Nat Biotechnol* 29, 24–26.

570 Shama, L.N.S., Wegner, K.M., 2014. Grandparental effects in marine sticklebacks: transgenerational
571 plasticity across multiple generations. *J. Evol. Biol.* 27, 2297–2307.
572 <https://doi.org/10.1111/jeb.12490>

573 Smit, P., AFA, Hubley, R.& Green, 2015. RepeatMasker Open-4.0.

574 Sun, X., He, Y., Hou, L., Yang, W.-X., 2010. Myosin Va participates in acrosomal formation and nuclear
575 morphogenesis during spermatogenesis of Chinese mitten crab *Eriocheir sinensis*. *PLoS One*
576 5, e12738. <https://doi.org/10.1371/journal.pone.0012738>

577 Tani, M., Ito, M., Igarashi, Y., 2007. Ceramide/sphingosine/sphingosine 1-phosphate metabolism on
578 the cell surface and in the extracellular space. *Cell. Signal.* 19, 229–237.
579 <https://doi.org/10.1016/j.cellsig.2006.07.001>

580 Teymouri Zadeh, Z., Shariatmadari, F., Sharafi, M., Karimi Torshizi, M.A., 2020. Amelioration effects of
581 n-3, n-6 sources of fatty acids and rosemary leaves powder on the semen parameters,
582 reproductive hormones, and fatty acid analysis of sperm in aged Ross broiler breeder
583 roosters. *Poult. Sci.* 99, 708–718. <https://doi.org/10.1016/j.psj.2019.12.031>

584 Tocher, D.R., Fonseca-Madrugal, J., Dick, J.R., Ng, W.-K., Bell, J.G., Campbell, P.J., 2004. Effects of
585 water temperature and diets containing palm oil on fatty acid desaturation and oxidation in
586 hepatocytes and intestinal enterocytes of rainbow trout (*Oncorhynchus mykiss*). *Comp.*
587 *Biochem. Physiol. B Biochem. Mol. Biol.* 137, 49–63.
588 <https://doi.org/10.1016/j.cbpc.2003.10.002>

589 Van Tran, L., Malla, B.A., Kumar, S., Tyagi, A.K., 2017. Polyunsaturated Fatty Acids in Male Ruminant
590 Reproduction - A Review. *Asian-Australas. J. Anim. Sci.* 30, 622–637.
591 <https://doi.org/10.5713/ajas.15.1034>

592 Velkova, M., Silva, N., Dello Stritto, M.R., Schleiffer, A., Barraud, P., Hartl, M., Jantsch, V., 2021.
593 *Caenorhabditis elegans* RMI2 functional homolog-2 (RMIF-2) and RMI1 (RMH-1) have both
594 overlapping and distinct meiotic functions within the BTR complex. *PLoS Genet.* 17,
595 e1009663. <https://doi.org/10.1371/journal.pgen.1009663>

596 Wang, H., Wan, H., Li, X., Liu, W., Chen, Q., Wang, Y., Yang, L., Tang, H., Zhang, X., Duan, E., Zhao, X.,
597 Gao, F., Li, W., 2014. Atg7 is required for acrosome biogenesis during spermatogenesis in
598 mice. *Cell Res.* 24, 852–869. <https://doi.org/10.1038/cr.2014.70>

599 White-Cooper, H., Bausek, N., 2010. Evolution and spermatogenesis. *Philos. Trans. R. Soc. B Biol. Sci.*
600 365, 1465–1480. <https://doi.org/10.1098/rstb.2009.0323>

601 Wu, H., Xu, T., Feng, H., Chen, L., Li, B., Yao, B., Qin, Z., Jin, P., Conneely, K.N., 2015. Detection of
602 differentially methylated regions from whole-genome bisulfite sequencing data without
603 replicates. *Nucleic Acids Res* 43, e141.

604 Yefimova, M.G., Buschiazzi, A., Burel, A., Lavault, M.-T., Pimentel, C., Jouve, G., Jaillard, S., Jegou, B.,
605 Bourmeyster, N., Ravel, C., 2019. Autophagy is increased in cryptorchid testis resulting in
606 abnormal spermatozoa. *Asian J. Androl.* 21, 570–576. https://doi.org/10.4103/aja.aja_12_19

607 Young, M.M., Wang, H.-G., 2018. Sphingolipids as Regulators of Autophagy and Endocytic Trafficking.
608 Adv. Cancer Res. 140, 27–60. <https://doi.org/10.1016/bs.acr.2018.04.008>
609 Zakrzewski, P., Rędownicz, M.J., Buss, F., Lenartowska, M., 2020. Loss of myosin VI expression affects
610 acrosome/acroplaxome complex morphology during mouse spermiogenesis†. Biol. Reprod.
611 103, 521–533. <https://doi.org/10.1093/biolre/ioaa071>
612 Zhao, J., Liu, T., Jin, S., Wang, X., Qu, M., Uhlén, P., Tomilin, N., Shupliakov, O., Lendahl, U., Nistér, M.,
613 2011. Human MIEF1 recruits Drp1 to mitochondrial outer membranes and promotes
614 mitochondrial fusion rather than fission. EMBO J. 30, 2762–2778.
615 <https://doi.org/10.1038/emboj.2011.198>
616

617

618

619

620

621

622

623

624

625

626

627

628

629

630

631

632

633

634

Tissue	Fish	Total raw reads	Trimmed reads	% of mapping	BS conversion (%)	Nuclear					Mitochondrial	
						Average CpG sequencing depth (x)	% CpGs covered 1x	% CpGs covered 5x	% CpGs covered 10x	CpG methylation (%)	Average CpG sequencing depth (x)	CpG methylation (%)
Muscle 12°C	1	324 054 890	312 036 061	60,16	99,35	11,02	93,38	78,93	54,04	78,13	2152,99	1,03
	2	314 187 112	301 636 081	58,86	99,38	10,46	92,47	77,44	50,38	74,80	2122,71	0,95
	3	323 609 587	313 382 478	60,34	99,36	11,24	92,59	78,67	54,56	74,47	2534,55	0,78
	4	346 904 275	334 318 944	60,55	99,37	12,05	93,06	79,82	58,62	75,70	3314,62	0,75
				59,98	99,37	11,19	92,88	78,71	54,40	75,77	2531,22	0,88
Sperm 12°C	1	300 587 067	294 303 143	59,66	99,15	10,58	92,29	77,88	50,85	88,41	74,09	7,65
	2	325 691 293	321 065 565	61,02	99,42	11	92,52	78,78	54,54	88,32	77,54	6,98
	3	336 626 182	332 307 052	61,31	99,39	11,54	92,57	79,35	56,11	88,47	62,51	5,23
	4	309 900 540	305 834 179	46,18	99,48	8,97	92,11	71,22	37,33	88,74	75,62	5,66
	5	332 585 217	326 170 573	59,67	99,50	11,07	92,76	78,98	54,21	88,25	39,75	11,90
	6	306 207 661	301 165 523	60,48	99,38	10,68	92,29	77,88	50,85	88,49	29,34	9,80
				58,05	99,39	10,64	92,43	76,81	49,71	88,45	59,81	7,87
Sperm 16°C	7	340 298 820	335 329 836	61,66	99,39	11,14	92,77	79,58	56,22	88,43	34,56	15,56
	8	309 013 645	304 553 951	60,67	99,40	10,71	92,71	78,56	52,32	88,71	113,23	5,21
	9	313 593 505	307 126 184	60,35	99,34	10,81	92,68	78,64	52,58	88,46	123,90	4,62
	10	311 388 841	305 315 136	61,97	99,35	11,17	92,51	78,71	54,59	88,77	76,70	4,12
	11	336 389 118	330 578 540	60,27	99,40	11,37	92,64	79,30	55,42	88,62	74,01	7,00
	12	311 912 118	306 606 582	60,73	99,36	11,03	92,59	78,91	54,24	88,61	54,91	5,06
				60,94	99,37	11,04	92,65	78,95	54,23	88,60	79,55	6,93

Tab 1. Summary of WGBS

Paired reads were mapped uniquely to the rainbow trout genome (Omik_1.0) using Bismark. Average sequencing depth. indicates the mean number of reads per position in nuclear and mitochondrial genomes. The nuclear coverage represents the proportion of mapped CpGs over the total number of CpG sites in the nuclear genome, here calculated under 1X, 5X or 10X sequencing depth selection threshold.

635

636

637

638

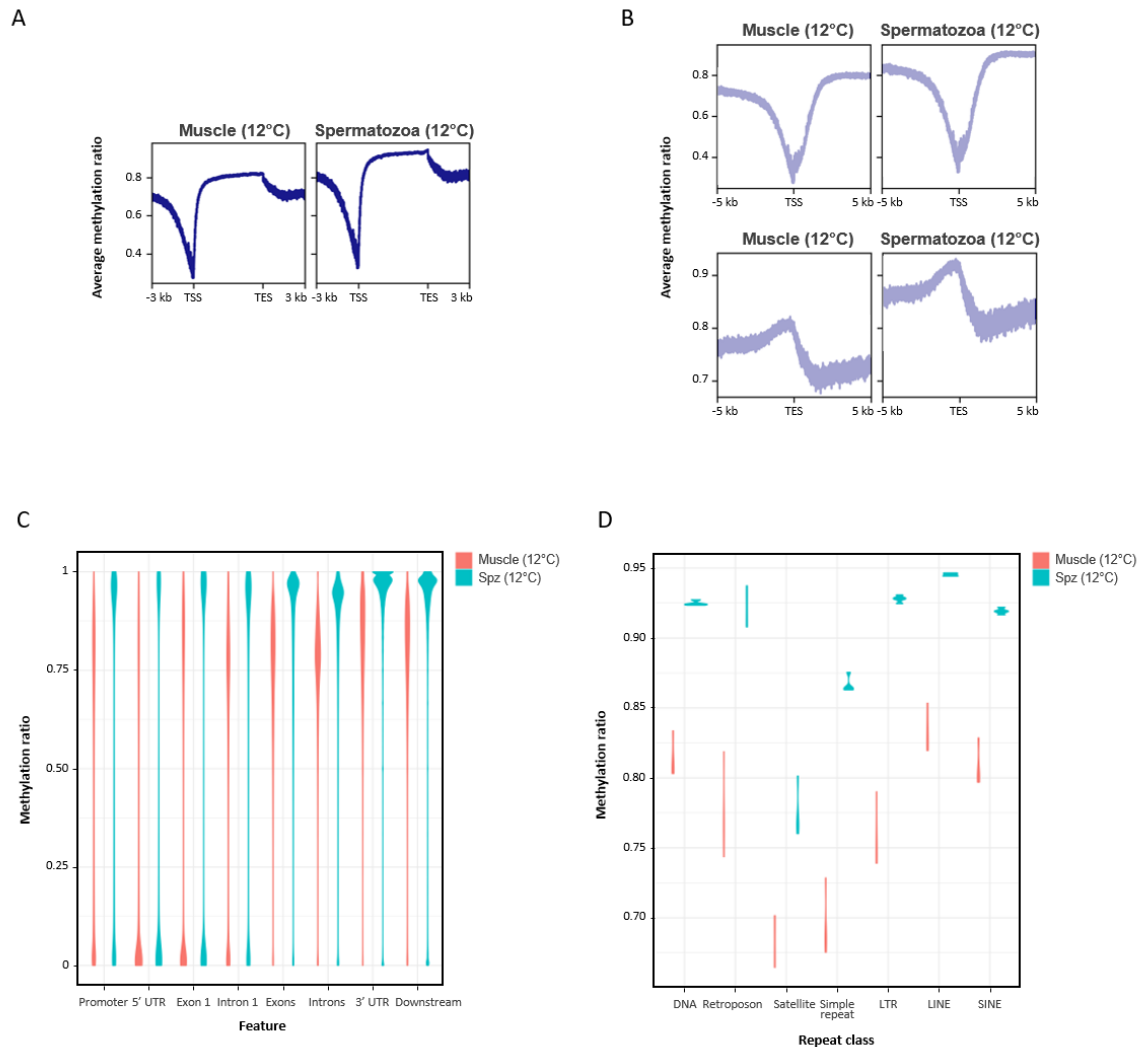
639

640

641

642

643



644

645

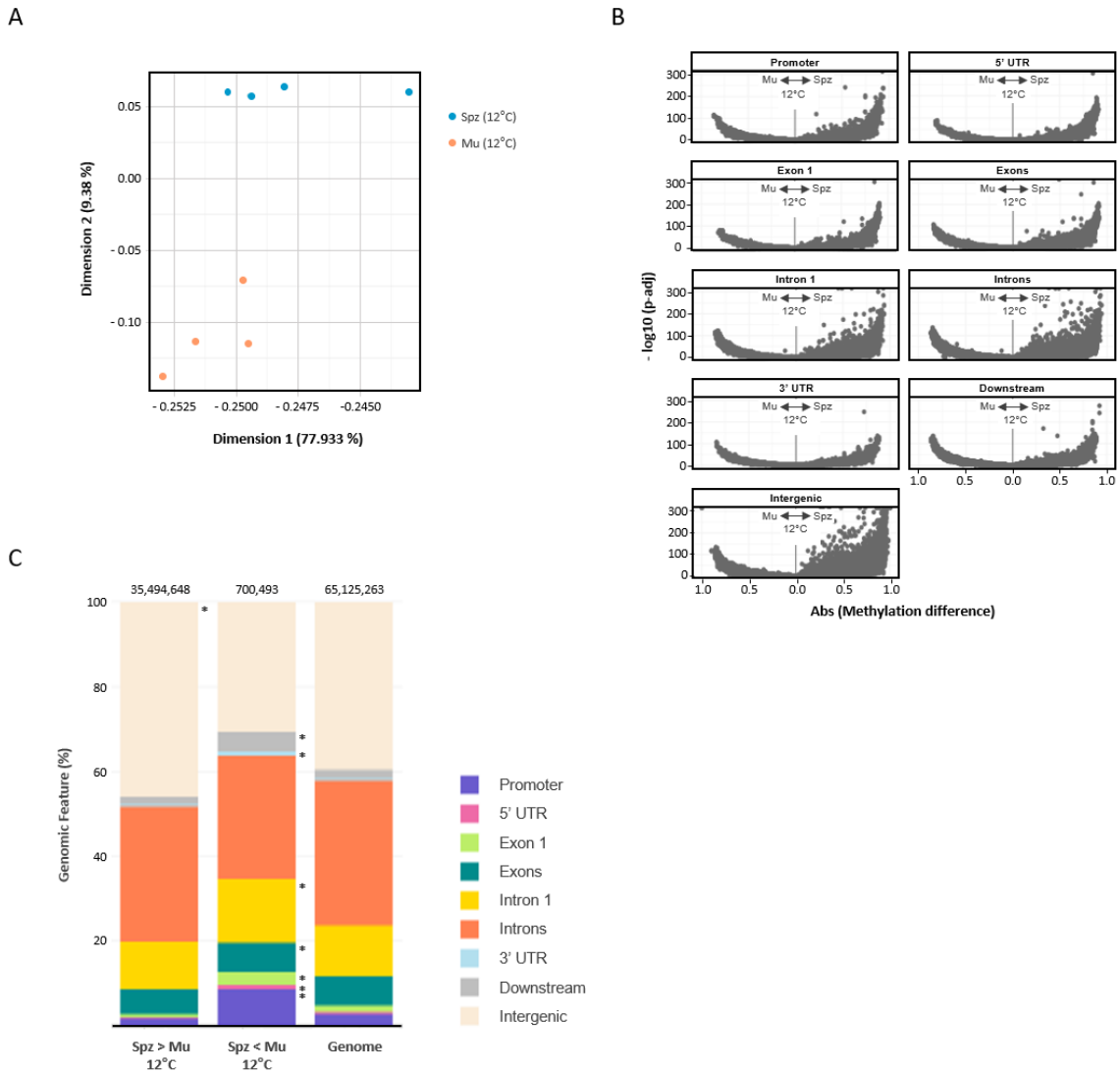
646 **Fig 1. Global DNA methylation in rainbow trout control muscle and spermatozoa according to**
 647 **genomic features**

648 A. Average methylation profiles along the 115 853 annotated ensembl coding and non-coding
 649 transcripts of ensembl v104 Omyk_1.0 genome. B. Average methylation profiles around TSS (+/- 5 kb)
 650 (left panels) and TES (+/- 5 kb) (right panels). C. Distribution of methylation ratios according to gene
 651 features: promoter regions (-1 kb ; TSS), 5'UTR, exon1, intron1, all exons, all introns, 3'UTR and
 652 downstream regions (TES ; +1 kb). D. Distribution of methylation ratios found in muscle and sperm in
 653 transposons (DNA), retroposons, satellites, simple repeats, LTR containing elements, LINEs and SINEs.

654

655

656



658

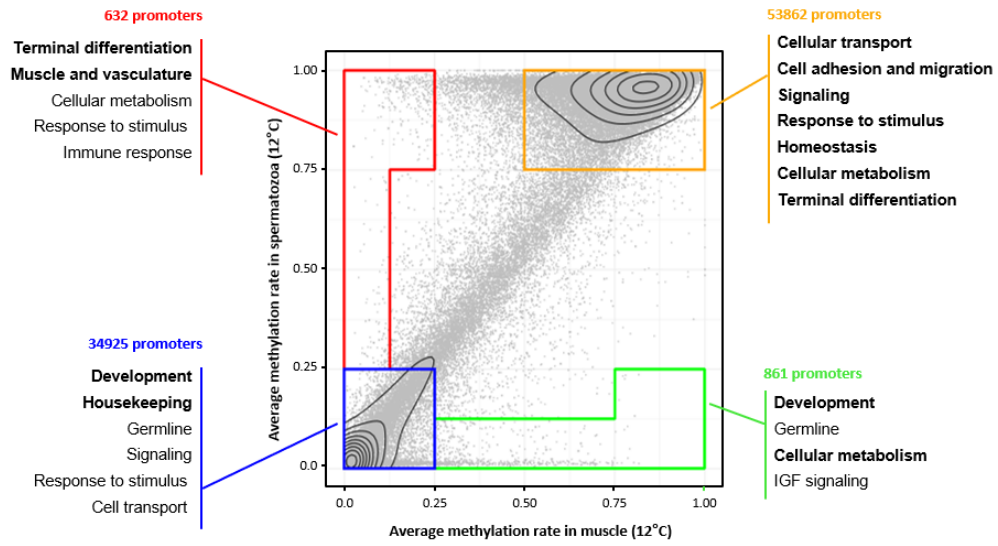
659 Fig 2. Differentially methylated cytosines between control spermatozoa and muscle

660 A. PCA plot of spermatozoa and muscle WGBS data sets. B. Volcano plots of DMCs between
 661 spermatozoa and muscle in every genomic feature (x axis : absolute methylation difference, y : $-\log_{10}$
 662 (adjusted p-value)). C. Relative distributions of DMCs (Spz > Mu : hypermethylated in sperm
 663 compared to muscle; Spz < Mu : hypomethylated in sperm compared to muscle) according to
 664 genome features (promoter regions (-1 kb ; TSS), 5'UTR, exon1, intron1, all exons, all introns, 3'UTR,
 665 downstream (TES ; +1 kb) and intergenic regions). The reference set (Genome) contains all analyzed
 666 CpGs. Genome features statistically enriched in DMCs compared to the reference set are indicated
 667 with an * (binomial test).

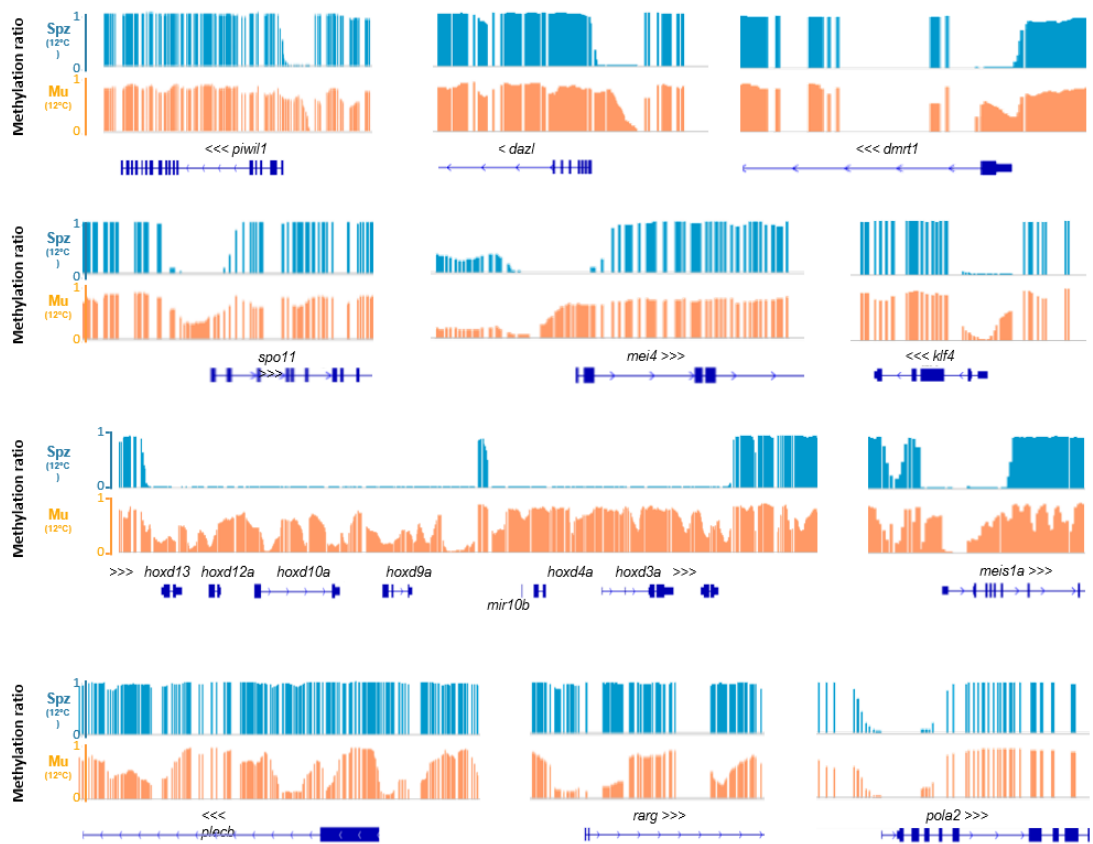
668

669

A



B



672

673 **Fig 3. Differentially methylated gene promoters between control spermatozoa and muscle**

674 A. Plot of average methylation of ensembl omyk_1.0 v105 transcripts promoters in muscle (x axis)
675 versus spermatozoa (y axis). Common hypo-methylated promoters are highlighted in the blue
676 square, common hyper-methylated promoters in the orange shape, muscle-specific hypo-
677 methylated promoters in the red shape and spermatozoa-specific promoters in the green shape.
678 Functional annotation terms deduced from a GO term enrichment analysis and corresponding to
679 each class are indicated. B. IGB snapshots of transcripts or TSS regions as examples of spermatozoa-
680 specific hypo-methylated promoters (*piwil1*, *dazl*, *dmrt1*, *spo11*, *mei4*, *hox* cluster and *mir10b*,
681 *meis1a*), muscle-specific hypo-methylated promoters (*plecb* and *rarg*) or common hypo-methylated
682 promoter (*pola2*). Muscle : Mu; Spermatozoa : Spz.

683

684

685

686

687

688

689

690

691

692

693

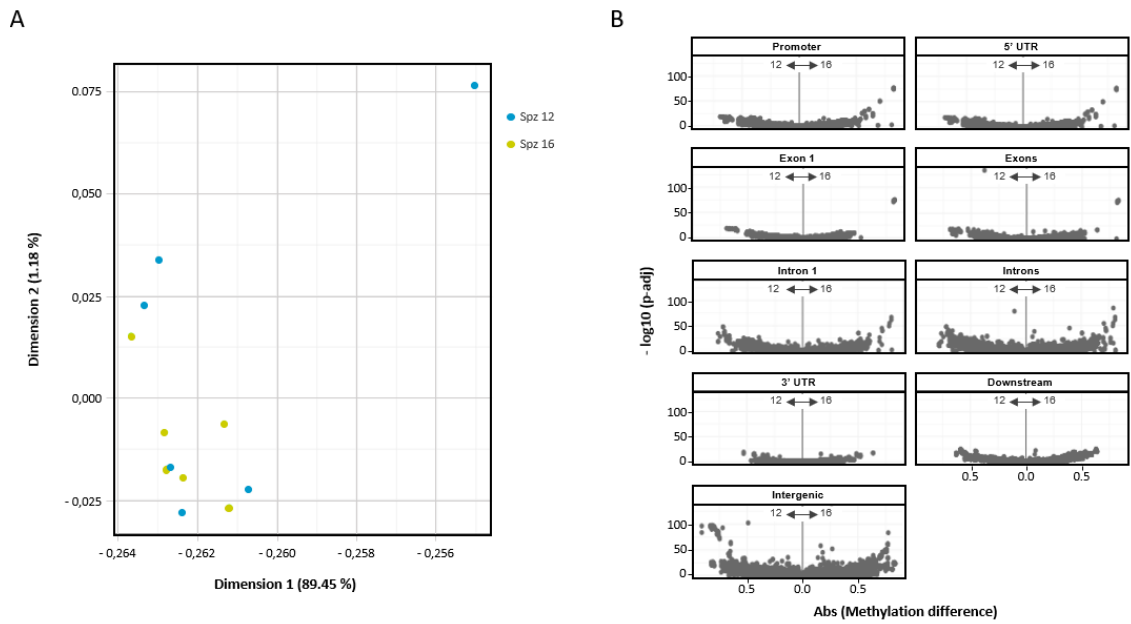
694

695

696

697

698



700

701 **Fig 4. Differentially methylated cytosines between spermatozoa from males raised at 16°C versus**
 702 **12°C**

703 A. PCA plot of spermatozoa from males raised at 12°C and 16°C WGBS data sets. B. Volcano plots of
 704 DMCs between spermatozoa from males raised at 12°C versus 16°C in every genomic feature (x axis :
 705 absolute methylation difference, y : -log10 (adusted p-value)).

706

707

708

709

710

711

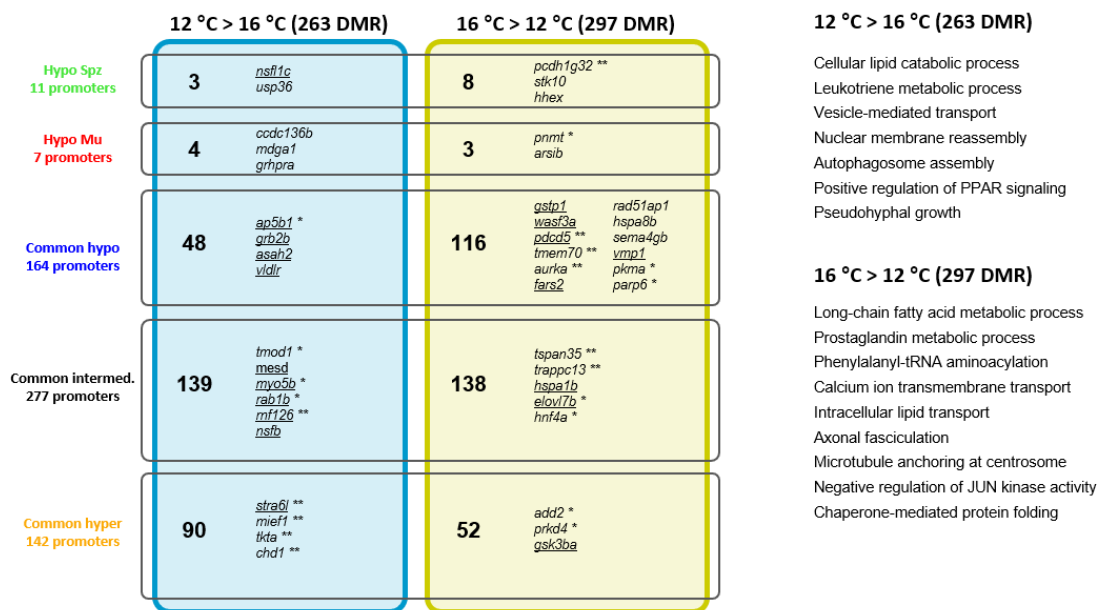
712

713

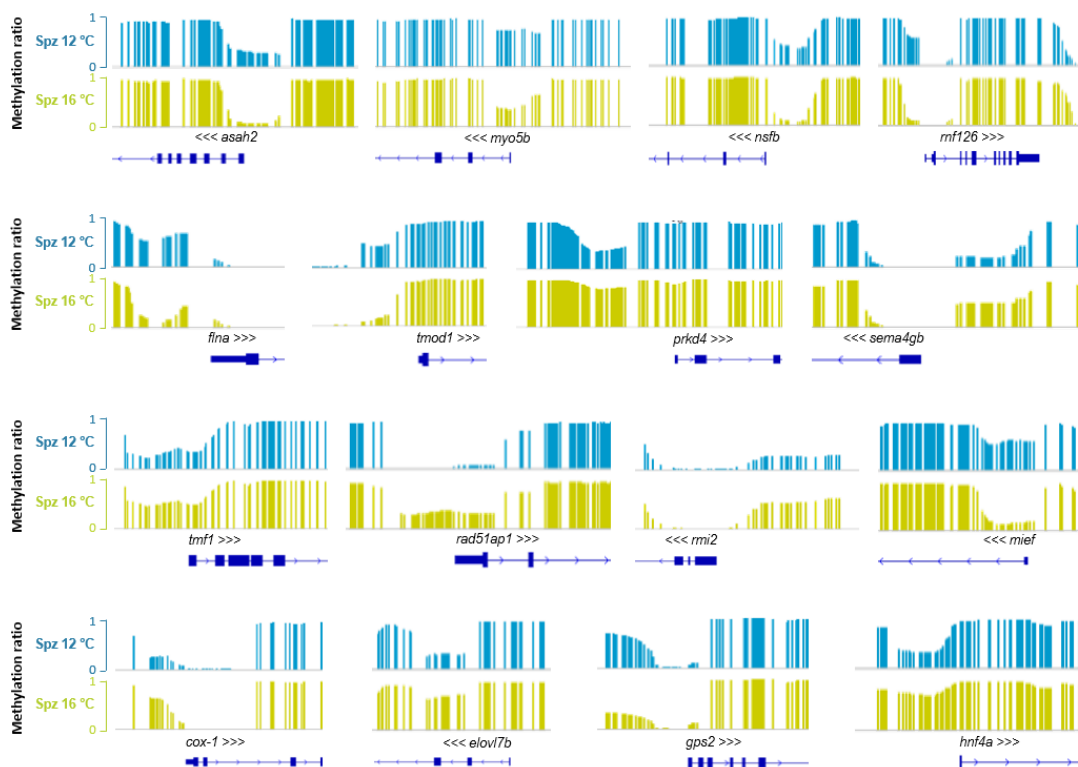
714

715

A



B



719 **Fig 5: Differentially methylated gene promoters between spermatozoa of fish raised at 16°C versus**
720 **12°C**

721 A. Intersection of up- and down-regulated DMRs with the different promoter categories defined in
722 Fig 3 (sperm-specific hyper or hypo-methylated, equally methylated,...) and associated GO term
723 enrichment analysis. Genes are given of examples of each categories, chosen either for their
724 association to an enriched GO term or for their presence in the top200 list of prom-DMRs.
725 underlined: associated to an enriched GO terms, *: top 10, **: top 50 prom-DMR. B. IGV snapshots of
726 TSS regions as examples of hyper- and hypo-methylated promoters at 16°C versus 12°C.

727

728

729

730

731

732

733

734

735

736

737

738

739

740

741

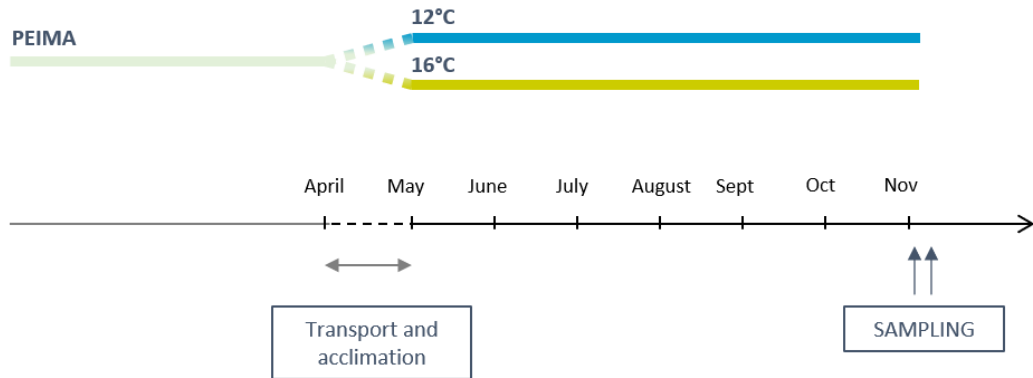
742

743

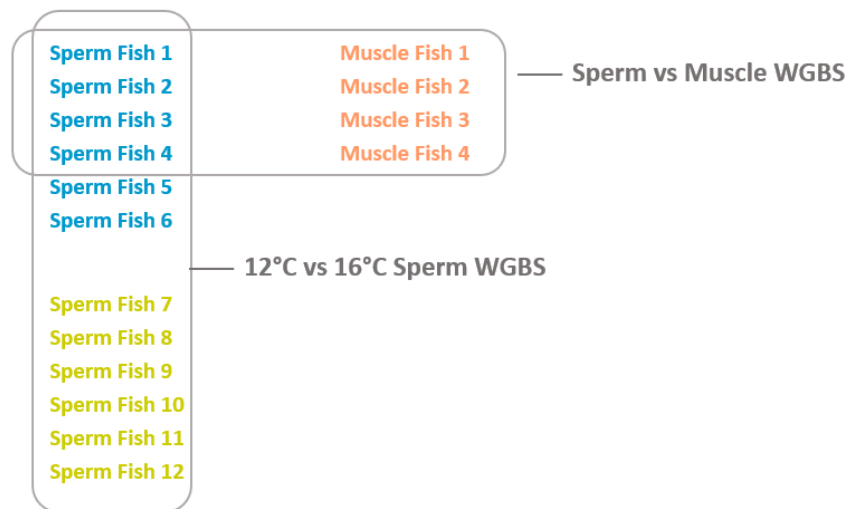
744

745

A



B



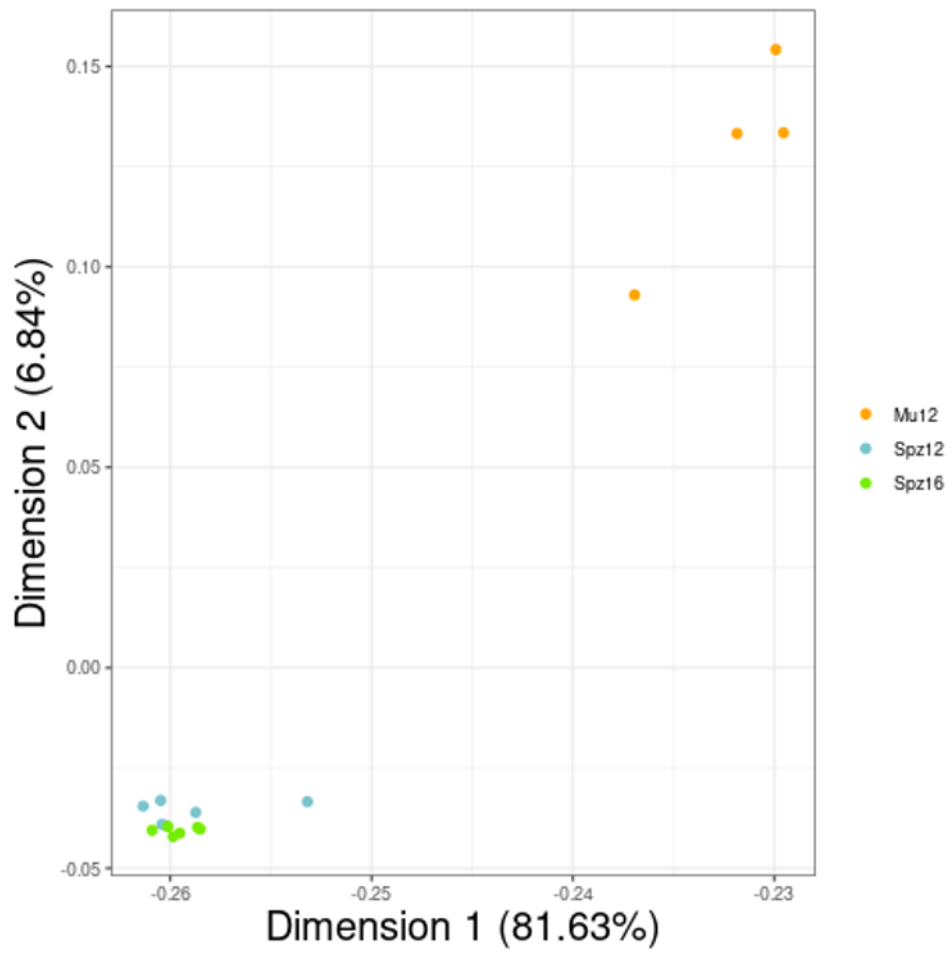
746

747

748 **Suppl Fig 1. Experimental design**

749 A. *Oncorhynchus mykiss* rainbow trouts were reared in our experimental farm and transferred to our
 750 indoor fish facility in April of their second year. Two groups of 20 males were kept in a recycling
 751 system, under artificial spring/summer/autumn photoperiod, and at the temperatures of 12°C and
 752 16°C (after 2 weeks acclimation and gradual temperature increase). Fish sperm and muscle were
 753 sampled during the reproduction period. B. Four fish were sequenced for the sperm versus muscle
 754 paired analysis while two groups of 6 fish were sequenced for the study of the temperature contrast
 755 in spermatozoa.

756



757

758

759 **Suppl Fig 2. PCA plot of muscle (Mu12), spermatozoa from males raised at 12°C (Spz12) and**
760 **spermatozoa from males raised at 16°C (Spz16) WGBS data sets**

761

762

763

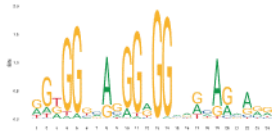
764

765

766

767

PRDM9 p-val 9.28e-35



768

769 **Suppl Fig 3. Putative recombination hotspots enrichment in DMRs between spermatozoa from**
770 **males raised at 16°C versus 12°C.**

771 Vertebrate PRDM9 consensus DNA binding site identified by MEME in DMR sequences between
772 spermatozoa from males raised at 16°C versus 12°C, and associated p-value.

773 MEME suite is accessible online (<https://meme-suite.org/meme/>), SEA algorithm was used.

774

775

776

777

778

779

780

781

782

783

784

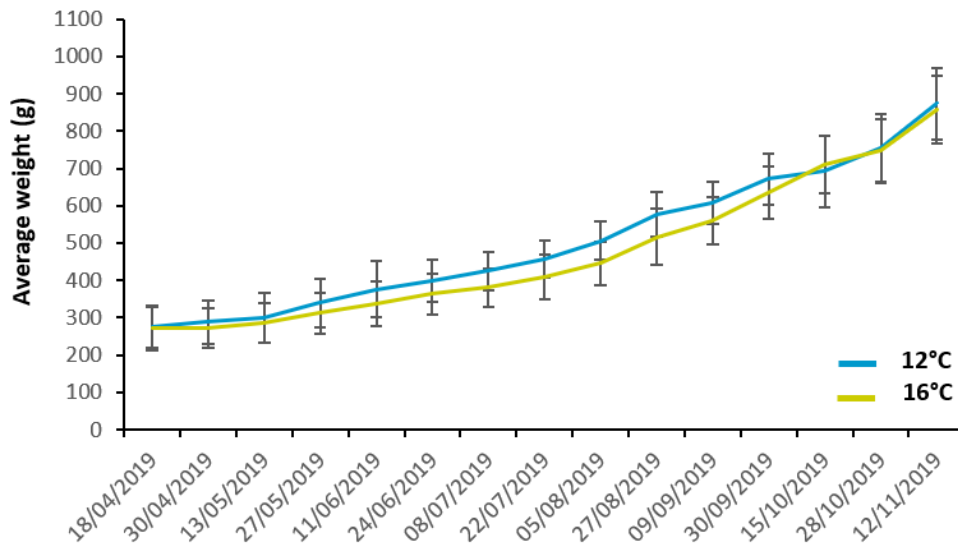
785

786

787

788

Weight of fish raised at 12°C and 16°C from April 18th to November 12th 2019



789

790

791 **Suppl Fig 4. Evolution of the weight of the fish raised at 12°C and 16° during the exposure to the**
792 **temperature increase.**

793 Fish weight was individually recorded every 2 weeks. The graph shows the weight averages and
794 standard deviations found for each group between April 18 and November 12 2019.

795